High-Temperature Reactions of O + COS and S + SO_2. Abstraction versus Substitution Channels

Nobuyasu Isshiki,[†] Yoshinori Murakami,[‡] Kentaro Tsuchiya,[§] Atsumu Tezaki,*[,†] and Hiroyuki Matsui[||]

Department of Mechanical Engineering, The University of Tokyo, Tokyo 113-8656, Department of Chemistry, Nagaoka University of Technology, Nagaoka Niigata 940-2188 Japan, National Institute of Advanced Industrial Science and Technology, Ibaraki 305-8565 Japan, and Department of Ecological Engineering, Toyohashi University of Technology, Toyohashi 441-8580, Japan

Received: January 11, 2002; In Final Form: January 7, 2003

The main concern of this study is to investigate the reaction mechanism of O + COS → products (1). Experiments are conducted by use of an excimer laser photolysis shock tube technique, where mixtures of COS and SO_2 diluted in Ar are photolyzed behind reflected shock waves. Time-resolved measurements of O and S atoms are conducted by use of atomic resonance absorption spectroscopy, and the overall rate constant of (1) is determined by the O atom decay at temperatures 1250−1600 K, i.e., $k_1 = 10^{-10.18\pm0.26}$ exp[−(22.5 ± 7.1) kJ·mol^{-1}/RT] cm^3 molecule^{-1} s^{-1}, which is in good agreement with the former recommendation. It is confirmed in this experiment that the S atom is a direct product of reaction 1. By analysis of time profiles of the S atom, the branching fraction of the S production channel O + COS → S + CO_2 (1b), α, is determined against the main channel O + COS → CO + SO (1a), where the S atom consumption reactions, S + SO_2 → 2SO (2) and S + COS → S_2 + CO (3), are inevitably taken into account. The present experimental result is expressed as $\alpha = (0.40 \pm 0.10) - (202 \pm 137)/T$ (T = 1120−1540 K). Also, in this kinetic analysis, the rate constant of (2) is simultaneously determined to be $k_2 = 10^{-11.01\pm0.33}$ exp[−(37.8 ± 8.2) kJ·mol^{-1}/RT]. The reaction mechanism of (1) is examined by comparing the experimental results with those of ab initio potential energy surface/transition state theory calculations.

Introduction

The current kinetic database for compounds containing sulfur is considerably immature compared to those of hydrocarbons and nitrogen compounds, even though combustion chemistry involving sulfur has been a considerable concern in a variety of modeling and kinetic studies.[1−6] Recently, a number of key elementary reactions related to the oxidation of H_2S, such as O + H_2S, H_2S pyrolysis, S + H_2, S + H_2S, HS + O_2, S + O_2, and SO + O_2, have been reinvestigated using a shock tube ARAS (atomic resonance absorption spectrometry) technique.[7−14] As a consequence of these studies, reconstruction of the reaction scheme in combustion modeling containing sulfur is strongly recommended, because new product channels and/or the alteration of the recommended kinetic rates was suggested in many of the above reactions.

As a continuation of the series study of high-temperature sulfur chemistry, this paper targets the reactions

$$O(^3P) + COS \rightarrow SO + CO \quad (1a)$$

$$O(^3P) + COS \rightarrow S + CO_2 \quad (1b)$$

In addition, the rate constant for the reaction

$$S(^3P) + SO_2 \rightarrow SO + SO \quad (2)$$

is simultaneously examined. As far as we have searched, the present study supplies a directly measured rate of this elementary reaction for the first time.

The overall rate constant for reaction 1 has been determined by a number of experiments in the temperature range of 239−1900 K, and they are mostly within a small deviation from the recommendation by Singleton and Cvetanovic[15] of

$$k_1 = 7.80 \times 10^{-11} \exp(-21.8\ \text{kJ·mol}^{-1}/RT)\ \text{cm}^3\ \text{molecule}^{-1}\ \text{s}^{-1}$$

The high-temperature data, however, are scarce. There has been a shock tube study conducted by Kruger and Wagner at around 1900 K[16] as well as discharge flow tube studies conducted by Homann et al. below 1150 K[17] and by Westenberg and DeHaas[18] below 808 K. Kruger and Wagner observed the O atom in shock-heated N_2O/COS mixtures and determined k_1 at 1900 K by the analysis of a complex reaction mechanism in which thermal decompositions of N_2O and COS take place simultaneously. The product channel of (1) is considered to be predominantly the abstraction (1a) at around room temperature and below. The substitution channel (1b) may contribute at higher temperatures, as Homann et al. observed CO_2 formation by the mass-spectrometric measurement. It is stated in Singleton's review that Topaloglu[19] monitored the relative rates of CO/CO_2 in his thesis work of shock tube oxidation of COS and estimated the rate of (1b) to be

* Corresponding author. Phone/fax: +81-3-5841-6293. E-mail: tezaki@comb.t.u-tokyo.ac.jp.
[†] The University of Tokyo.
[‡] Nagaoka University of Technology.
[§] National Institute of Advanced Industrial Science and Technology.
[||] Toyohashi University of Technology.

10.1021/jp0200829 CCC: $25.00
Published on Web 03/13/2003

$$k_{1b} = 8.30 \times 10^{-11} \exp(-46.0 \pm 8.3\ \text{kJ·mol}^{-1}/RT)\ \text{cm}^3\text{·molecule}^{-1}\ \text{s}^{-1}$$

$$T = 1200-1900\ \text{K}$$

Accordingly, the branching fraction to (1b) is estimated to be about 10% at 1200 K.

Reaction 2 is a reversible process, in which the forward step is endothermic ($\Delta H°_f = 31.8$ kJ/mol).[4] Although this has been suggested as one of the essential reactions responsible for the conversion of SO_2 into S_2 in flames,[4] there has been no convincing experimental result for (2) at high temperatures within our search. Just and Rimpel[20] assumed a rate constant of (2) in the analysis of a complex reaction mechanism describing their shock tube experiment of SO_2 decomposition. Because only the equilibrium relationship between S, SO_2, and SO is essential in their experimental condition, they did not examine the rate constant in detail.

Schofield[4] cited an estimate for the reverse reaction as

$$k_{-2} = 1.0 \times 10^{-12} \exp(-1720/T)\ \text{cm}^3\ \text{molecule}^{-1}\ \text{s}^{-1}$$

which has an experimental validation only at room temperature. This reaction is important to equilibrate S_2 and SO_2 at combustion temperature; however, a number of studies led to only upper limits,[21] and a discharge flow tube result of Martinez and Herron[22] seems to be the only dependable data.

The former shock tube studies for these reactions employed conventional thermal excitation techniques; i.e., reactions began with pyrolysis of stable species. This requires a complex reaction analysis, whereas the sensitivity to the successive concerned reaction is not necessarily high. Consequently, it seems worth conducting an up-to-date shock tube study combined with a pulsed photolysis as a prompt and selective excitation method.

After searching proper sample conditions, we found that reactions 1 and 2 concurrently take place in the analyzable relationship at photolysis of COS/SO_2 mixtures behind shock waves. Rate constants of (1) and (2), as well as the product branching ratio of (1), have been obtained through the analysis.

In addition, the experimental rate constants and the branching fraction of (1) in the present work were compared with theoretical values derived based upon the G2M methodology and the transition-state theory.

Experimental Section

A newly constructed shock tube apparatus has been used in this study, whereas the basic design is essentially the same as that used in our previous studies,[7−11] except for small modifications of dimensions. The shock tube is composed of a diaphragmless high-pressure section and a 4 cm i.d., 4 m long low-pressure section that has a quartz window at the end. S(^{3}P) and O(^{3}P) atoms were detected by using ARAS. For the S atom detection, 0.1% SO_2 diluted in He was flowed in a microwave discharge lamp to generate the resonance radiation at 182.6 nm, and the light transmitted through the shock tube was monitored with a VUV monochromator (Ritsu, MCV-20, 20 cm focal length) and a solar-blind photomultiplier (Hamamatsu, R976). The O atom was detected in the same way, using 1% O_2 diluted in He in the lamp to generate the radiation at 130.5 nm. An excimer laser (Lambda Phisik, LPX100) operated in KrF mode (248 nm) is placed face-to-face to the tube end to photolyze precursor molecules in shock-heated sample gas filled in the low-pressure section. Usually, the laser was triggered at100 μs after the arrival of a reflected shock wave at the observation section. Pulse energy of the excimer laser was monitored at every shock by detecting scattered light from the quartz window with a photodiode calibrated preliminarily. Typical fluence of the laser pulse was 60 mJ/cm^2 at the front of the entrance window. Width of the laser beam overlapping the absorption path is restricted to 3.5 cm at the window to avoid irradiation to the inner wall of the tube.

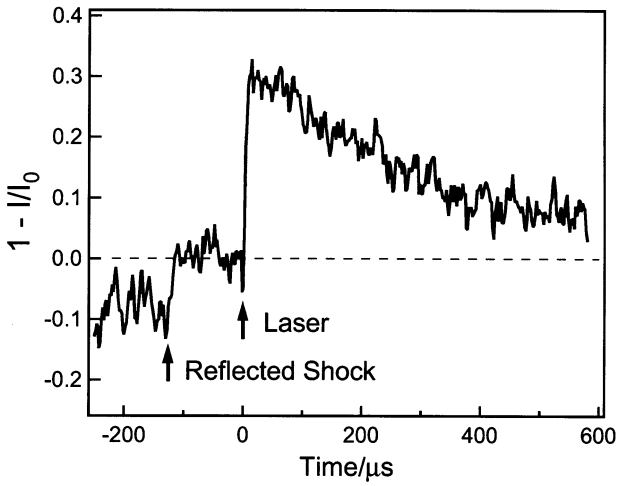

Figure 1. Typical O atom profile in KrF laser photolysis of COS/SO_2 mixtures behind a reflected shock. $[COS]/[SO_2] = 40/100$ ppm, $T_5 = 1576$ K, $\rho_5 = 6.6 \times 10^{18}$ molecules/cm^3.

The low-pressure section was evacuated to ca. 1×10^{-6} Torr by a turbomolecular pump prior to filling the sample gas. COS was purified by a trap-to-trap distillation. Research grade SO_2 supplied in a glass ampule was used without further purification. Ar (research grade) was purified by passing through a cold trap before use.

It was indicated in previous studies[8,10,11] that the effective absorption coefficient of S(^{3}P) atom in the ARAS measurement is practically independent of temperature but dependent on total density. According to the established procedure, the absorption of S was calibrated by thermal decomposition of COS at 2700−3500 K at several densities covering the present conditions. The results showed slight deviations from the Lambert−Beer law at absorbance up to 1 in the total density range of $2.5-9.5 \times 10^{18}$ molecules/cm^3. O(^{3}P) atom absorption is known to be independent of density[7,10] and was calibrated by thermal decomposition of N_2O at 2700−3300 K. In the present experiment, photolysis in the mixtures of COS/SO_2 resulted in simultaneous production of S(^{3}P) and O(^{3}P) atoms, whose initial concentrations were evaluated using these calibration curves.

Results and Discussion

Overall Rate Constant of O + COS. The overall rate constant of O + COS (1) has been determined straightforwardly by analyzing O atom decay in the COS/SO_2 mixtures. As shown in Figure 1, the O atom is produced instantly at the irradiation of laser pulse, and then it decays single exponentially. The photon energy of 248 nm is less than that of the bond dissociation energy of SO_2 (threshold wavelength is 217 nm). Nevertheless, intense radiation from a KrF excimer laser yields O(^{3}P) production, probably due to the successive photon absorption via the electronic excited state of SO_2. If so, production of O (^{1}D) atom in the 248 nm photolysis of SO_2

TABLE 1: Reaction Rate Constants Used in the Present Analysis

		rate constant $AT^n \exp(-E/RT)$			
no.	reaction	A/(cm^3 molecule^{-1} s^{-1})	n	E/kJ·mol^{-1}	remarks, refs
1a	O + COS = CO + SO	6.6×10^{-11}		22.5	$k_{1overall}$, this study
1b	O + COS = S + CO_2	$k_{1b}/k_1 = 0.40-202/T$			this study
2	S + SO_2 = SO + SO	9.8×10^{-12}		37.8	this study
3	S + COS = S_2 + CO	4.9×10^{-11}		31.0	96SHI/OYA, ref 11
4	O + SO_2 = SO + O_2	8.3×10^{-12}		81.5	88SIN/CVE, ref 15
5	SO_2 + M = SO + O + M	4.7×10^{-08}		487	78JUS/RIM, ref 20
6	SO + M = S + O + M	6.6×10^{-10}		448	84PLA/TRO[a]
7	S + O_2 = SO + O	2.5×10^{-11}		15.3	97TSU/KAM, ref 7
8	O+ S_2 = SO + S	2.2×10^{-11}		0.70	87CRA/MUR[b]
9	O_2 + M = O+ O + M	3.0×10^{-06}	−1	494	86TSA/HAM[c]
10	COS = CO + S	4.1×10^{-10}		257	94OYA/SHI, ref 9
11	S_2 + M = S + S + M	8.0×10^{-11}		322	80HIG/SAI[d]

[a] Plach, H. J.; Troe, J. *Int. J. Chem. Kinet.* **1984**, *16*, 1531. [b] Craven, W.; Murrell, J. N. *J. Chem. Soc., Faraday Trans. 2* **1987**, *83*, 1733. [c] Tsang, W.; Hampson, R. F. *J. Phys. Chem. Ref. Data* **1986**, *15*, 1087. [d] Higashihara, T.; Saito, K.; Murakami, I. *Bull. Chem. Soc. Jpn.* **1980**, *53*, 15.

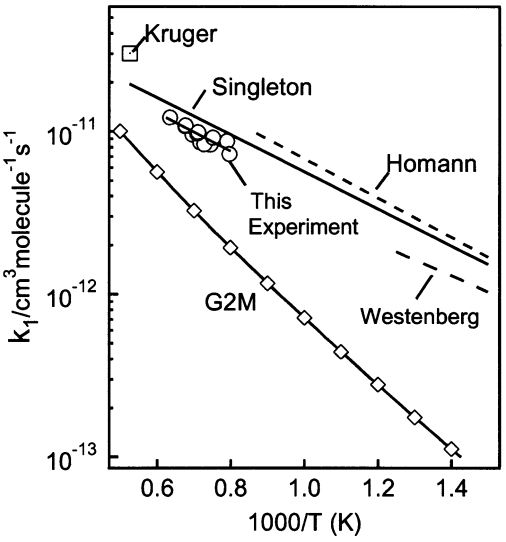

Figure 2. Comparison of overall rate constant O + COS (1) between this experiment, literature, and transition state theory (TST) calculations based on G2M theoretical PES.

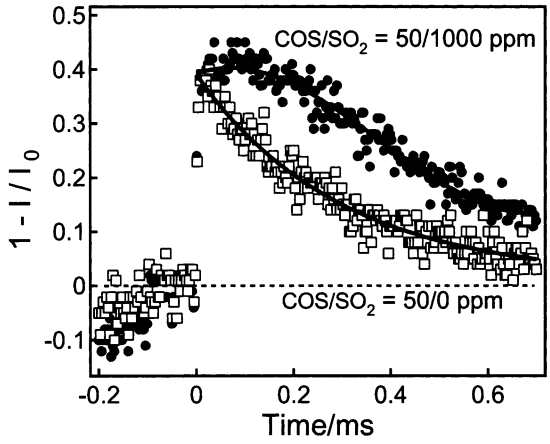

Figure 3. S atom profiles in the photolysis of COS with and without SO_2 at $T_5 = 1600$ K, $\rho_5 = 1.15 \times 10^{19}$ molecules/cm^3. The laser pulse is at $t = 0$. Solid circles, 50 ppm COS with 1000 ppm SO_2; open rectangles, 50 ppm COS without SO_2.

may also be possible, however, the O(^{1}D) quenching to the ground O(^{3}P) is sufficiently fast (about 10^{-7} s in the present shock tube conditions) to avoid unnecessary reactions in concern. The second-order rate constants for (1) were obtained by use of known COS concentration, and the results are shown in Figure 2 together with reported rate constants. The photodecomposition of COS was estimated to be negligible, and the reaction rate of O + SO_2 is known to be sufficiently slow.[15]

A least-squares fit of the present experimental data in the temperature range of 1250−1600 K gives

$$k_1 = 10^{-10.18\pm0.26} \exp[-(22.5 \pm 7.1)\ \text{kJ·mol}^{-1}/RT]\ \text{cm}^3\ \text{molecule}^{-1}\ \text{s}^{-1}$$

(All indicated error limits are two times statistical standard deviations.)

As shown in Figure 2, the present results are in good agreement with extrapolation of the previous experimental results at lower temperatures. Although our result is below Singleton's recommendation by 20%, the deviation is well within the stated error limit of 50% in the review. The activation energies are also in very good agreement with each other. The shock tube result by Kruger and Wagner[16] is above these lines, and they suggested a possibility of curved Arrhenius behavior at a higher temperature range, which is not apparent in the present result.

Analysis of S Atom Observations. Figure 3 shows a typical example of S atom profiles in the photolysis of COS with and without addition of SO_2. In the case without SO_2, the S atom is promptly produced at the laser incidence and then simply decays in single exponential manner. This decay is predominantly governed by S + COS reaction, and the decay rates were in excellent agreement with our former publications.[9,11] In the case with SO_2 coexistence, the S atom shows further increase after photolysis, followed by slower decay. Initial rise rate of the S atom is consistently accounted for by O atom consumption in reaction 1, assuming that the S atom is a direct product of (1) against various conditions conducted in this experiment. The decay part of the S atom is regarded as consumption by the reactions S + SO_2 (2) and S + COS (3).

Numerical analyses were conducted to find rate parameters to reproduce the observed profiles of the S (^{3}P) atom. The reaction mechanism used in this analysis is given in Table 1. Only reactions 1−4 are important in this analysis, but other reactions are included in Table 1 for completeness. Among these additional reactions, O + S_2 (8) has the most significant contribution (up to 4% to the decay of O atom at typical experimental conditions). Because the overall rate constant for (1) has been already determined in the previous section and reliable rate constants for (3) and (4) are available, k_2 and the branching fraction $\alpha = k_{1b}/k_1$ are left to be determined. These two parameters, however, were not determined uniquely in a single experiment as shown in Figure 4. Namely, increasing k_2 by 20% and decreasing α by 20% have almost identical effects to the simulated curve, although each of them has a

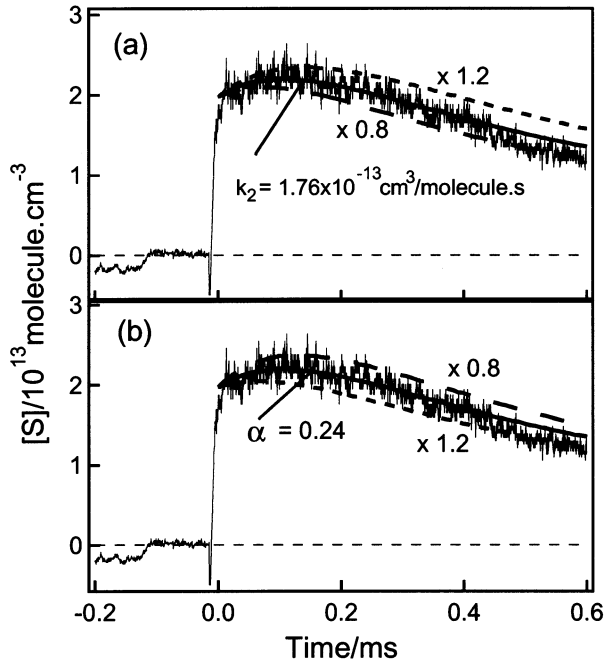

Figure 4. Comparisons between an experimental S atom profile and those of numerical simulations demonstrating sensitivities to the rate constant of S + SO_2 (2) and the branching fraction $\alpha = k_{1b}/k_1$ in the present kinetic mechanism. $T = 1220$ K, $\rho_5 = 5.8 \times 10^{18}$ molecules/cm^3, [COS]/[SO_2] = 50/4000 ppm. In the simulations, $k_2 = 1.76 \times 10^{-13}$ cm^3 molecule^{-1} s^{-1} and $\alpha = 0.24$ at the best fit, then k_2 and α are varied ±20% in (a) and (b), respectively.

considerable sensitivity to the profile of the S atom. Accordingly, we have conducted the following procedure to determine these two values. In the experiments, three different samples of COS/SO_2 ratios (50/1000, 50/2000, and 50/4000 ppm/ppm) were prepared, and S atom profiles were acquired in the same temperature and density range for these samples. A series of data having different sample conditions at close temperature were compared to calculated profiles using a certain pair of k_2 and α to find the best combination of the two parameters. In this way, these could be determined unambiguously at each series of data. These results are summarized in Figures 5 and 6. The branching fraction α obtained by this procedure has been fitted to the following relationship:

$$\alpha = k_{1b}/k_1 = (0.40 \pm 0.10) - (202 \pm 137)/T$$

$$T = 1120-1540 \text{ K}$$

This gives 0.2−0.3 at 1200 K, nearly twice that of the former evaluation,[14] and is close to its indicated upper uncertainty limit. The nature of these branching channels will be discussed further in the next section.

The rate constant for (2) obtained in this study is shown in Figure 5 with a former estimate. A least-squares fit for the present rate constant determination for (2) gives

$$k_2 = 10^{-11.01\pm0.33} \exp[-(37.8 \pm 8.2) \text{ kJ·mol}^{-1}/RT] \text{ cm}^3 \text{ molecule}^{-1} \text{ s}^{-1}$$

$$T = 1120-1540 \text{ K}$$

As shown in the figure, the present result of k_2 is in remarkable agreement with the conversion of the recent evaluation of the reverse SO + SO rate suggested by Schofield,[4] whereas the former assumption used by Just and Rimpel[20] is one order higher

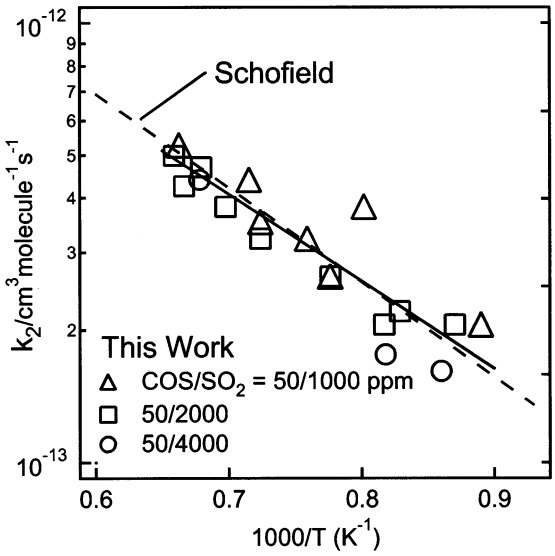

Figure 5. Arrhenius plot of the overall rate constant of S + SO_2 (2). Symbols are experimental results of this work, and a solid line is the least-squares fit. A dashed line is a conversion of Schofield's estimate for the rate of reverse reaction 4.

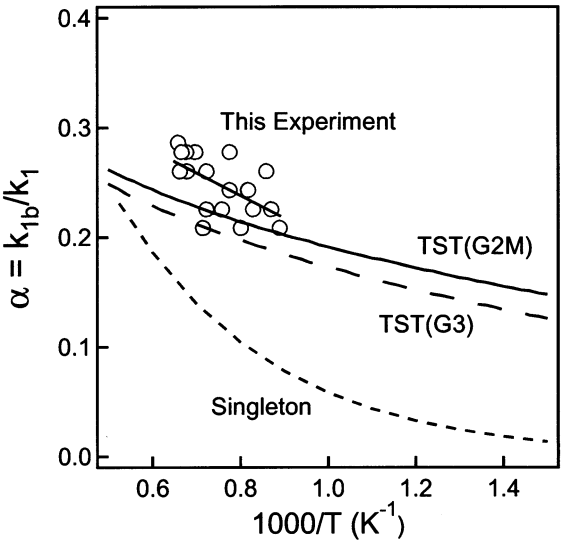

Figure 6. Arrhenius plot of the branching fraction to the S + CO_2 product channel (1b) in the O + COS reaction. Open circles are determined from present experiment. Lines are those from Singleton's review[15] and TST calculations using G2M and G3 potential energies.

than these results. The parameters given by Just seem to be a combination of a typical preexponential factor of bimolecular reactions and an activation energy equal to the endothermic reaction enthalpy, and as already described, the rate probably has no significant sensitivity to their simulation. The Schofield evaluation is an extrapolation from room-temperature data of a flow tube experiment[21] using his former evaluation of the thermochemical data of this reaction.[20]

The activation energy for (2) obtained here is greater than the reaction enthalpy (31.8 kJ/mol) by 6 kJ mol^{-1}: if this energy difference corresponds to the barrier height of the reverse process (−2), the present value is considerably smaller than that indicated by Schofield (about 14 kJ mol^{-1}). The discrepancy of the activation energies of the reverse process is canceled by the difference of the indicated preexponential factors.

Theoretical Calculation for the O + COS Reaction. Gaussian 98 code[23] was used for the PES calculations for the triplet O−S−C−O system. All molecular structures, including

TABLE 2: Rotational Constants and Vibrational Frequencies of a Reactant, Products, Transition States, and an Intermediate in the O(^{3}P) + OCS System Calculated at the B3LYP/Aug−cc−pVTZ Level

	rotational constants/GHz	vibrational frequency/cm^{-1}	ZPE[a]/kJ mol^{-1}
TS1 (^{3}A″)	17.61, 3.72, 3.07	323i, 119, 431, 495, 811, 2078	23.1
TS2a (^{3}A″)	9.62, 5.95, 3.68	398i, 267, 442, 522, 792, 2071	24.0
TS2b (^{3}A′)	10.98, 5.52, 3.67	659i, 283, 409, 634, 771, 1984	23.9
SCO_2 ($^3A_1$)	14.59, 5.05, 3.75	279, 482, 567, 721, 998, 1441	26.3
OCS	6.07	527, 527, 873, 2107	23.7
CO	58.15	2207	12.9
CO_2	11.73	674, 674, 1369, 2400	30.0
SO	21.13	1150	6.7

[a] The values of ZPE were calculated with the scaling factor of 0.98.

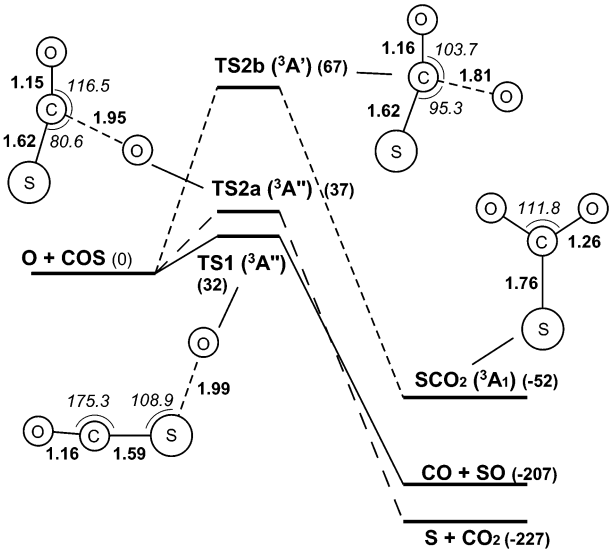

Figure 7. Potential energies and geometries of transient species in the O(^{3}P) + OCS system calculated at the B3LYP/aug-cc-pVTZ/G2M level of theory. Bond distances in angstroms and angles in degrees are described by bold and italic numbers, respectively. Numbers in parentheses next to state characters are enthalpies at 0 K relative to O + COS in the unit of kJ/mol. The vertical scale of the diagram is not in exact scale.

those for transition states, were optimized using the B3LYP hybrid density functional method[24,25] and the cc-pVTZ basis set. Figure 7 shows geometries, including three transition states found in this calculation. TS1 is apparently the transition state of the abstraction channel (1a), and two other ones are possibly transition states of the substitution channel 1b, namely, TS2a with ^{3}A″ electronic state and TS2b with ^{3}A′ electronic state. The former was found to correlate directly to S(^{3}P) + CO_2, and the latter was found to correlate to bound SCO_2 with $^3A_1$ electronic state that readily dissociates to S(^{3}P) + CO_2 via internal conversion into repulsive ground $^3B_2$ electronic state. Calculated rotational constants and vibrational frequencies are listed in Table 2. Classical barrier heights relative to reactants for these competitive channels were estimated by the G2M(CC1)[26] and G3[27,28] methodology, with zero-point energy correction obtained by the density functional method. As shown in Table 3, relative barrier heights between the three transition states are nearly the same in the two methods, although the absolute values obtained by the latter are lower by ca. 9−11 kJ·mol^{-1} compared to those by the former. It is shown that TS2b is considerably higher than the other two transition states; hence, it can be neglected among the effective reaction pathways. Consequently, TS2a is attributed to the right TS of the substitution channel.

The conventional transition state theory[29] with the Wigner tunneling correction[30] was used to calculate rate constants for each channel. The calculated rate constant is shown in Figure 2, and the branching fractions are plotted in Figure 6 compared with present experimental results. Although the absolute overall rate constants in the two methodologies are lower than the experimental ones and differ from each other, the branching ratios are fairy close, reflecting the agreement of relative TS heights, and are consistent with the present experimental result. The calculated overall rate constants exhibit increasing activation energy with increasing temperature, mainly due to the thermal nature of partition functions, rather than the increasing contribution of the substitution channel. However, the predicted curvature of the Arrhenius plot is not apparent enough to be experimentally evidenced at the current temperature range.

TABLE 3: Enthalpies at 0 K of the Intermediate, Products, and Transition States, Relative to O(^{3}P) + OCS (in kJ mol^{-1})

	G2M(CC1)	CCSD-based G3[a]	experimental
TS1 (^{3}A″)	31.6	20.7	
TS2a (^{3}A″)	37.4	27.5	
TS2b (^{3}A′)	66.7	58.1	
SCO_2 ($^3A_1$)	−52.4	−53.0	
SO + CO	−206.6	−210.8	−214[b]
S(^{3}P) + CO_2	−227.0	−221.1	−223[b]

[a] Spin-projected MPn energies were employed instead of unprojected MPn ones. [b] Atkinson, R.; Baulch, D. L.; Cox, R. A.; Hampson, R. F., Jr.; Kerr, J. A.; Troe, J. *J. Phys. Chem. Ref. Data* **1992**, *21*, 1125.

Conclusions

By use of the excimer laser photolysis in shock tube experiments, the complexity of the reaction mechanism was considerably reduced compared to the previous thermal excitation experiments, although simultaneous production of S and O atoms in the photolysis in the COS/SO_2 mixtures brought some indirect analytic procedure. The overall rate constant of O + COS (1) was determined directly by analyzing profiles of O without having significant disturbance from secondary reactions and is consistent with former studies conducted at different temperature ranges. The product branching fraction forming S + CO_2 was derived by analyzing profiles of the S atom. The estimated branching fraction for the substitution channel was consistent with ab initio/TST theoretical calculations.

The rate constant of S + SO_2 (2) was simultaneously determined by analyzing profiles of the S atom. Other than the present result, there seem to be no dependable data at elevated temperature range so far. As this is a simple reaction in which the spin conservation rule is held, the observed Arrhenius *A* factor might be too small (10^{-11} cm^3 molecule^{-1} s^{-1}). In the successive study over extended temperature range, it is suggested that the Arrhenius plot is nonlinear, to give a reasonable magnitude for the *A* factor. Detailed discussion will be presented elsewhere.[31]

References and Notes

(1) Fenimore, C. P.; Jones, G. W. *J. Phys. Chem.* **1965**, *69*, 3593.

(2) Durie, R. A.; Johnson, G. M.; Smith, M. Y. *Combust. Flame* **1971**, *17*, 197.

(3) Kallend, A. S. *Combust. Flame* **1972**, *19*, 227.

(4) Schofield, K. *Combust. Flame* **2001**, *124*, 137.

(5) Mischler, B.; Beaud, P.; Gerber, T.; Tzannis, A.-P.; Radi, P. P. *Combust. Sci. Technol.* **1996**, *119*, 375.

(6) Radi, P. P.; Mischler, B.; Schlegel, A.; Tzanninis, A.-P.; Beaud, P.; Gerber, T. *Combust. Flame* **1999**, *118*, 301.

(7) Tsuchiya, K.; Kamiya, K.; Matsui, H. *Int. J. Chem. Kinet.* **1997**, *29*, 57.

(8) Shiina, H.; Miyoshi, A.; Matsui, H. *J. Phys. Chem. A* **1998**, *102*, 3556.

(9) Oya, M.; Shiina, H.; Tsuchiya, K.; Matsui, H. *Bull. Chem. Soc. Jpn.* **1994**, *67*, 2311.

(10) Tsuchiya, K.; Yokoyama, K.; Matsui, H.; Oya, M.; Dupre, G. *J. Phys. Chem.* **1994**, *98*, 8419.

(11) Shiina, H.; Oya, M.; Yamashita, K.; Miyoshi, A.; Matsui, H. *J. Phys. Chem.* **1996**, *100*, 2136.

(12) Shiina, H.; Miyoshi, A.; Matsui, H. *J. Phys. Chem. A* **1998**, *102*, 3556.

(13) Woiki, D.; Roth, P. *J. Phys. Chem.* **1994**, *98*, 12958.

(14) Olschewski, H. A.; Troe, J.; Wagner, H. Gg. *J. Phys. Chem.* **1994**, *98*, 12964.

(15) Singleton, D. L.; Cvetanovic, R. J. *J. Phys. Chem. Ref. Data* **1988**, *17*, 1377 and references therein.

(16) Kruger, B.; Wagner, H. Gg. *Z. Phys. Chem., Neue Folge* **1981**, *126*, 1.

(17) Homann, K. H.; Krome, G.; Wagner, H. Gg. *Ber. Bunsen-Ges. Phys. Chem.* **1968**, *72*, 998.

(18) Westenberg, A. A.; DeHaas, N. *J. Chem. Phys.* **1969**, *50*, 707.

(19) Topaloglu, T. *Diss. Abst. Int., B* **1982**, *42*, 4134.

(20) Just, Th.; Rimpel, G. *Proc. 11th Int. Symp. Shock Tubes and Shock Waves* **1978**, 226.

(21) Schofield, K. *J. Phys. Chem. Ref. Data* **1973**, *2*, 25.

(22) Martinez, R. I.; Herron, J. T. *Int. J. Chem. Kinet.* **1983**, *15*, 1127.

(23) Frisch, M. J.; Trucks, G. W.; Schlegel, H. B.; Scuseria, G. E.; Robb, M. A.; Cheeseman, J. R.; Zakrzewski, V. G.; Montgomery, J. A., Jr.; Stratmann, R. E.; Burant, J. C.; Dapprich, S.; Millam, J. M.; Daniels, A. D.; Kudin, K. N.; Strain, M. C.; Farkas, O.; Tomasi, J.; Barone, V.; Cossi, M.; Cammi, R.; Mennucci, B.; Pomelli, C.; Adamo, C.; Clifford, S.; Ochterski, J.; Petersson, G. A.; Ayala, P. Y.; Cui, Q.; Morokuma, K.; Malick, D. K.; Rabuck, A. D.; Raghavachari, K.; Foresman, J. B.; Cioslowski, J.; Ortiz, J. V.; Stefanov, B. B.; Liu, G.; Liashenko, A.; Piskorz, P.; Komaromi, I.; Gomperts, R.; Martin, R. L.; Fox, D. J.; Keith, T.; Al-Laham, M. A.; Peng, C. Y.; Nanayakkara, A.; Gonzalez, C.; Challacombe, M.; Gill, P. M. W.; Johnson, B. G.; Chen, W.; Wong, M. W.; Andres, J. L.; Head-Gordon, M.; Replogle, E. S.; Pople, J. A. *Gaussian 98*, revision A.7; Gaussian, Inc.: Pittsburgh, PA, 1998.

(24) 4 Becke, A. D. *J. Chem. Phys.* **1993**, *98*, 5648.

(25) Lee, C.; Yang, W.; Parr, R. G. *Phys. Rev. B: Condens. Matter Mater. Phys.* **1988**, *37*, 785.

(26) Mebel, A. M.; Morokuma, K.; Lin, M. C. *J. Chem. Phys*. **1995**, *103*, 7414.

(27) 7 Curtiss, L. A.; Raghavachari, K.; Redfern, P. C.; Rassolov, V.; Pople, J. A. *J. Chem. Phys.* **1988**, *109*, 7764.

(28) Curtiss, L. A.; Raghavachari, K.; Redfern, P. C.; Baboul, A. G.; Pople, J. A. *Chem. Phys. Lett.* **1999**, *314*, 101.

(29) Steinfeld, J. I.; Francisco, J. S.; Hase, W. L. In *Chemical Kinetics and Dynamics*; Prentice-Hall: Englewood Cliffs, NJ, 1989.

(30) Wigner, E. P. *Z. Phys. Chem., Abt. B* **1932**, *19*, 203.

(31) Murakami, Y.; et al. In preparation.